Spatial variations in CO2 fluxes in a subtropical coastal reservoir of Southeast China were related to urbanization and land-use types

Spatial variations in CO_2 fluxes in a subtropical coastal reservoir of Southeast China were related to urbanization and land-use types

Yifei Zhang[1,2,3], Min Lyu[4], Ping Yang[1,2*], Derrick Y.F. Lai[5], Chuan Tong[1,2,], Guanghui Zhao[2], Ling Li[2], Yuhan Zhang[2], Hong Yang[6,7,8,***]**

[1]*Key Laboratory of Humid Subtropical Eco-geographical Process of Ministry of Education, Fujian Normal University, Fuzhou 350007, P.R. China*

[2]*School of Geographical Sciences, Fujian Normal University, Fuzhou 350007, P.R. China*

[3]*Key Laboratory of Wetland Ecology and Environment, Northeast Institute of Geography and Agroecology, Chinese Academy of Sciences, Changchun 130102, Jilin, P.R. China*

[4]*School of Urban and Rural Construction, Shaoyang University, Shaoyang 422000, China*

[5]*Department of Geography and Resource Management, The Chinese University of Hong Kong, Hong Kong, China*

[6]*College of Environmental Science and Engineering, Fujian Normal University, Fuzhou 350007, P.R. China*

[7]*Collaborative Innovation Center of Atmospheric Environment and Equipment Technology, Jiangsu Key Laboratory of Atmospheric Environment Monitoring and Pollution Control (AEMPC), School of Environmental Science and Engineering, Nanjing University of Information Science and Technology, Nanjing, 210044, China*

[8]*Department of Geography and Environmental Science, University of Reading, Reading, RG6 6AB UK*

***Corresponding authors**: Ping Yang (yangping528@sina.cn)

****Corresponding authors**: Chuan Tong (tongch@fjnu.edu.cn)

Telephone: 086-0591-87445659 **Fax:** 086-0591-83465397 **Email:** tongch@fjnu.edu.cn

*****Corresponding authors**: Hong Yang (hongyanghy@gmail.com)

Abstract

Carbon dioxide (CO_2) emissions from aquatic ecosystems are important components of the global carbon cycle, yet the CO_2 emissions from coastal reservoirs, especially in developing countries where urbanization and rapid land use change occur, are still poorly understood. In this study, the spatiotemporal variations in CO_2 concentrations and fluxes were investigated in Wenwusha Reservoir located in the southeast coast of China. Overall, the mean CO_2 concentration and flux across the whole reservoir were 41.85 ± 2.03 μmol/L and 2.87 ± 0.29 mmol/m^2/h, respectively, and the reservoir was a consistent net CO_2 source over the entire year. The land use types and urbanization levels in the reservoir catchment significantly affected the input of exogenous carbon to water. The mean CO_2 flux was much higher from waters adjacent to the urban land (5.05 ± 0.87 mmol/m^2/hr) than other land use types. Sites with larger input of exogenous substance via sewage discharge and upstream runoff were often the hotspots of CO_2 emission in the reservoir. Our results suggested that urbanization process, agricultural activities, and large input of exogenous carbon could result in large spatial heterogeneity of CO_2 emissions and alter the CO_2 biogeochemical cycling in coastal reservoirs. Further studies should characterize the diurnal variations, microbial mechanisms, and impact of meteorological conditions on reservoir CO_2 emissions to expand our understanding of the carbon cycle in aquatic ecosystems.

Keywords

Carbon dioxide fluxes; Spatiotemporal dynamics; Land use; Urbanization; Anthropogenic activities; Coastal reservoir

Introduction

Dams have been built for thousands of years to control water flow and utilize water resources (Nilsson et al., 2005). As an artificial aquatic ecosystem, reservoirs play an important role in irrigation, water supply, power generation, aquaculture and other aspects, while the impacts of such water projects on the local hydrological situation and ecosystem sustainability have not been fully explored (Hao et al., 2019; Rosenberg et al., 2000). With the inundation of land and vegetation in the reservoir area, nutrient transport and cycling in the flooded system will change substantially, with the consequence of changing the emission of greenhouse gases (GHGs), including CO_2, CH_4 and N_2O, into the atmosphere (Li et al., 2016; St Louis et al., 2000). Therefore, with the exacerbating climate change caused by increasing GHG concentrations (World Meteorological Organization, 2019), quantifying the carbon flux of reservoirs becomes increasingly important to improve the accuracy of carbon budget estimations from local to global scales.

Artificial reservoir, which includes various carbon sources from the catchment and inside the reservoir, is a major component of global carbon cycle (Bevelhimer et al., 2016; Kunz et al., 2011). Recent estimate indicates that global GHG emissions from reservoir water surfaces account to approximately 0.8 Pg CO_2-eq (100-year) per year, of which ~17% is contributed by CO_2 (Deemer et al., 2016). Reservoirs appear to be a net source of atmospheric CO_2 (Barros et al., 2011; Raymond et al., 2014), especially in the subtropical and tropical areas (e.g., Alshboul and Lorke, 2015; Almeida et al., 2019). CO_2 emissions from reservoirs on a per unit area basis tend to exceed those from natural lakes or wetlands. However, limited by the number of field observations available, these CO_2 estimates are largely uncertain (Li and Lu, 2012; Varis et al., 2012). More importantly, the spatial heterogeneity (across and within systems) caused by geographical location, reservoir age, microtopography, water temperature, organic matter, and other factors further pose challenges for the accurate estimate of CO_2 emissions from reservoirs.

Different from other natural water bodies, reservoirs have special ecosystem characteristics under the intervention of human activities (Fearnside, 2005; Soumis et al., 2007). Generally, the inundated sediment, suspended particles and other associated carbon trapped in reservoirs provide stable carbon sources for CO_2 production, but with large spatial heterogeneity (Hertwich, 2013; Kemenes et al., 2011; Zhou et al., 2017). On the other hand, some eutrophic waters with higher primary productivity can fix a large amount of CO_2, and even serve as a carbon sink for a certain period (Pacheco et al., 2015). Previous studies suggested several possible conditions for the dominance of autotrophic processes: (1) relatively enclosed and stagnant water environment (van Bergen et al., 2019); (2) warm and humid climate (Barros et al., 2011; Xiao et al., 2017); and (3) excessive import and accumulation of nutrients and organic matter in the reservoirs (Dodds and Cole, 2007; Outram and Hiscock, 2012). Furthermore, compared with inland areas, coastal reservoirs trend to have a higher salinity (Domingues et al., 2016; Hodson et al., 2019). CO_2 production and emission may also exhibit some spatial differences owing to variations in salinity.

With rapid urbanization and land use change in the coastal areas, various biogeochemical processes in the coastal aquatic ecosystems have been increasingly disturbed by municipal and agricultural activities in the catchment (Pérez et al., 2015; Williams et al., 2016), leading to the creation of critical “hotspots” of GHG emission (Yang and Flower 2012). High CO_2 production and emission in some river and lake systems have been shown to closely relate to the exogenous supply of sewage-derived organic matter from the watershed (e.g., Kaushal et al., 2018; Pugh et al., 2015). Coastal reservoirs, which can be affected by both terrestrial and marine ecosystems, are likely to exhibit unique CO_2 dynamics. Given that most

of the existing studies on CO_2 fluxes in reservoirs are mainly devoted to inland hydroelectric reservoirs only (e.g., Abril et al., 2005; Shi et al., 2017) but rapid urbanization occurs widely in the catchment of coastal reservoirs, particularly in the developing countries (Yang et al., 2017). Therefore, a deeper understanding about the influence of land use change and urbanization on CO_2 fluxes in the coastal reservoirs is needed.

Given the knowledge gap above, we measured CO_2 concentrations and fluxes in a subtropical coastal reservoir in Min River Estuary, Southeast China, from November 2018 to June 2019. The goals of this study were: (1) to assess the spatial variability of CO_2 concentration and flux in the subtropical coastal reservoir system, and (2) to determine the response of reservoir CO_2 release to the adjacent land use types. We hypothesized a large spatial heterogeneity in reservoir CO_2 fluxes because of the different land use types and urbanization levels in the catchment.

1. Materials and methods

1.1. Site description

This study was conducted in Wenwusha Reservoir (25°49′36″−25°54′00″N, 119°35′12″−119°38′11″E), which was located at the southern tip of the Min River Estuary, Southeast China (**Fig. 1**). The reservoir catchment is influenced by a subtropical monsoon climate with high temperature (annual average: 19.3 °C) and abundant precipitation (annual average: 1390 mm). Nearly 75% of the annual precipitation occurs from May to September (Yang et al., 2020). The reservoir water meets China's Class III water quality standard (suitable for centralized drinking water source protection zone, fish protection zone and swimming zone), and the reservoir is mainly used for irrigation, aquaculture and flood control (Fuzhou Municipal Water Authorities, 2019). Different species of fish, including *Lateolabrax japonicus, Oreochromis mossambicus, Carassius auratus auratus* and *Cyprinus carpio,* grow in the reservoir. The main land uses adjacent to the reservoir are urban area (5.99%), aquaculture pond (9.80%), forest (15.04%), farmland (3.34%), sand (2.14%) and wetland (14.41%) (**Fig. 1** and **Table 1**).

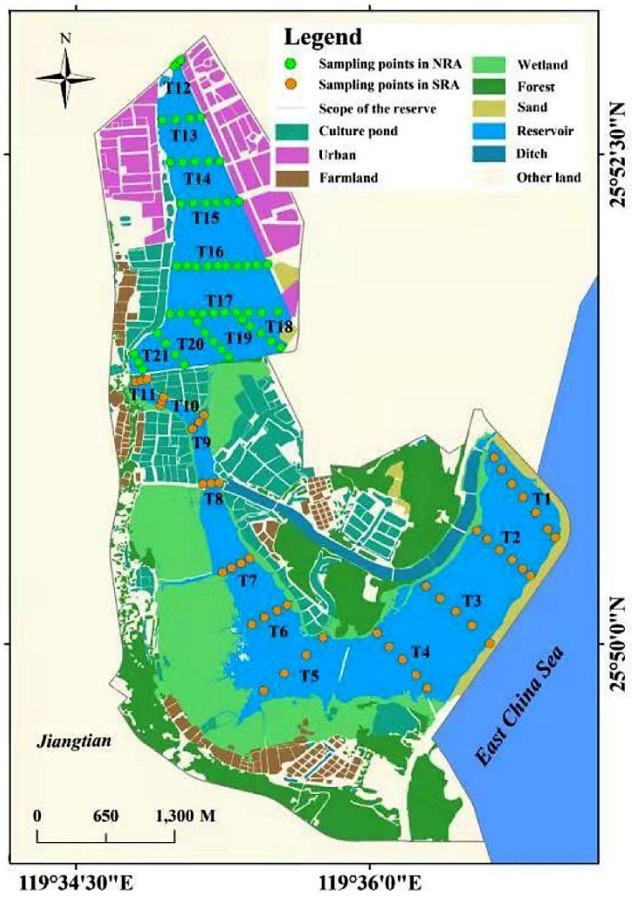

Fig. 1. Location of the Wenwusha Reservoir and land use distribution in the catchment. There are 11 sample transects (47 sampling sites) in the south reservoir area (SRA) and 10 sampling transects (56 sampling sites) in the north reservoir area (NRA).

Table 1

Summary of main characteristics and land use types in the Wenwusha Reservoir

	Surface area (ha)	Total volume ($\times 10^8$ m^3)	Water depth (m)	Bank type[a]	Sampling Site	Land use type (%)					
						Urban	Pond	Farmland	Wetland	Forest	Sand
NRA	190	1.4	2.6	N/C	56	23.93	6.30	2.01	0.01	0.34	1.41
SRA	330	1.69	1.2	N	47	0.00	10.96	3.78	10.96	19.94	2.39

[a]"N" and "C" represent natural and concreted banks. NRA and SRA are north reservoir area and sour reservoir area.

The total reservoir water area and mean water depth are 520 ha and 1.5 m, respectively. Two dams were built in 1957 and 2004, respectively, which divided the reservoir into two main reservoir areas: north reservoir area (NRA) and south reservoir area (SRA) (**Fig. 1**). The NRA, with a surface area of 190 ha, is connected to the Nanyang River network. Influenced by urbanization and human activities, the NRA and its upstream receive effluent discharge from domestic, industrial and aquacultural activities (**Table 1**). The construction of the southern seawall resulted in the SRA, with a surface area of 330 ha. Trees were planted in the east of SRA, while extensive wetlands were formed along the west bank of SRA with some agricultural landscapes (e.g., aquaculture ponds and farmlands) (**Table 1**). Water in the whole reservoir is supplied by precipitation and upstream river discharge, with almost no exchange with sea.

1.2. Water sampling and CO_2 measurement

Considering the possible spatiotemporal variations in dissolved CO_2 concentration and flux, three sampling campaigns (November 2018, March and June 2019) were carried out across 21 sampling transects (103 sites) at the Wenwusha reservoir, including 10 sampling transects in NRA (56 sites) and 11 transects in SRA (47 sites). Moreover, according to different levels of urbanization along the reservoir bank in the catchment, the reservoir was further divided into four water areas (I, II, III, and IV) (Appendix A **Table S1**). The sampling points basically covered all the water areas with the dominating land use types in the catchment (**Fig. 1**). The coordinates of each sampling site were recorded so that the same sites were re-visited in all three sampling campaigns. Water samples were collected using 55-mL borosilicate serum bottles (~0.2 m below the water surface), which were then sealed with butyl stoppers and aluminum caps without including any bubbles. In addition, 150-mL of water sample was collected at each site using a polyvinylchloride sampling bottle for the measurement of other auxiliary parameters (see below).

CO_2 concentration was determined using the headspace extraction technique (Bellido et al., 2009). Specifically, 25 mL of water sample and equal volume of N_2 were added into a bottle and the bottle was then violently shaken for 10 min to reach an equilibrium in CO_2 concentration. 5 mL of headspace air sample was collected and subsequently injected into a gas chromatograph (GC-2010, Shimadzu, Kyoto, Japan) with flame ionization detection (FID) for determining the CO_2 concentration. Four CO_2 standard gases, i.e. 100, 500, 1000 and 10,000 ppm, were used to calibrate the FID. The injection port, column and detector temperature were set at 100, 45 and 240 °C, respectively. Dissolved CO_2 concentration in water was calculated following the method of Wanninkhof (1992), based on the CO_2 concentration in the headspace air in the serum bottle and the Bunsen solubility coefficient.

The CO_2 flux (F_{CO2}) across the water-air interface was estimated using the thin-boundary layer model based on gas diffusion between two media (e.g., Crawford et al., 2013) as follows:(1)FCO2=k*(Cwater−Catm)where F_{CO2} (mmol/m²/h) refers to the CO_2 flux from water to air; k is the gas transfer velocity of CO_2 (m/hr); C_{water} is the CO_2 concentration in the water column (mmol/L), and C_{atm} is the CO_2 concentration in the atmosphere (mmol/L). In the lentic system, according to the empirical function driven by wind speed and temperature (Crusius and Wanninkhof, 2003), the k value can be calculated as:(2)k=(1.68+0.228*U102.2)*(600SC)n(3)SC=1991.1−118.11t+3.4527t2−0.04132t3where U_{10} (m/sec) is the wind speed at 10 m above the water surface, which is approximated by U_{10}= 1.14 U, where U is the wind speed at 2 m height; S_C is the CO_2 Schmidt number for water temperature (t, °C) (Wanninkhof, 1992); and n is the proportionality coefficient (value is 0.5).

1.3. Field and laboratory measurement of water physico-chemical properties

During the sampling period, various physio-chemical properties of surface water were also measured *in situ*. Water temperature (T_W) and pH were measured by a portable pH/mV/temperature meter system (IQ150 Scientific Instruments, USA). Dissolved oxygen (DO) and salinity were determined by a portable water quality analyzer (HORIBA, Japan) and a salinity meter (Eutech Instruments-Salt6, USA), respectively. The relative standard deviations of pH, DO, and salinity analyses were ≦1.0%, ≦2.0% and ≦1.0%, respectively. All equipment probes were calibrated following the manufacturer's specifications prior to deployment. Meteorological conditions (including wind speed, air pressure and temperature) were measured by a meteorological meter (NK3500, Kestrel, USA), and long-term precipitation data were obtained from the weather stations in Min River Estuary.

Laboratory analyses were conducted to determine the nutrient concentrations in reservoir water. Before the analysis of dissolved nutrients, water samples were filtered through 0.45–μm GF/F glass millipore filters. Dissolved organic carbon (DOC) concentration was analyzed by a total organic carbon analyzer (TOC-VCPH/CPN, Shimadzu, Japan) with a detection limit of 0.4 μg/L and a relative standard deviation (RSD) of ≤1.0% in 24 h. Nitrogen (total dissolved nitrogen (TDN), NO_3^-, and NH_4^+) and phosphorus (total phosphorus (TP) and PO_4^{3-}) nutrients were detected using flow injection analyzer (Skalar Analytical SAN^{++}, Netherlands). The detection limits for nitrogen and phosphorus were 6 μg/L and 3 μg/L, respectively, and the measurement reproducibilities were within 3.0% and 2.0%, respectively. Chlorophyll *a* (Chl-*a*) was extracted using ethanol solution (90%) for 24 h and analyzed by a UV–VIS spectrophotometer (Shimadzu UV-2450, Japan).

1.4. Statistical analysis

All measured variables were checked for normality using the Kolmogorov-Smirnov's test. When necessary, the original data were transformed by the natural logarithm to meet the assumptions of normality and homoscedasticity. To fully consider the correlation between spatial variables, as well as the randomness and structural characteristics of the spatial distribution of samples, the Kriging method in ArcGIS 10.2 (Esri, Redland, CA, USA) was employed for the spatial interpolation. Significant differences in CO_2 concentration, flux and environmental variables among different water areas were tested by analysis of variance (ANOVA). Spearman correlation and simple regression analysis were conducted to explore the relationships between CO_2 concentration (or flux) and the physio-chemical properties of water. Statistical significance was examined at the level of 0.05. The key factors influencing the CO_2 concentration and flux in the two reservoir areas were further investigated using redundancy analysis (RDA) in CANOCO 5.0 (Ithaca, NY, USA). Statistical results and graphics were generated by using SPSS 17.0 (IBM, Chicago, IL, USA) and Origin 2017 (OriginLab Corporation, USA), separately.

2. Results

2.1. Meteorological conditions and physico-chemical properties of reservoir water

The general spatiotemporal variations of surface water physico-chemical properties have been reported in Yang et al. (2020) (**Table 2** and Appendix A **Fig. S2**), while in this study, we focused on the effects of urbanization. Daily temperature, atmospheric pressure, wind speed, water salinity and Chl-*a* concentration showed small spatial variations, and the mean difference was less than 4 °C, 10 hPa, 3 m/s, 2‰ and 9 μg/L, respectively, during the research period. Spatially, water DO, TOC, TDN, NH_4^+, and PO_4^{3-} concentration varied

considerably among the four areas. TOC, NH_4^+ and TDN in Areas I and Area-II showed much higher concentrations than those in Area-III and Area-IV ($p < 0.05$ or 0.01; **Table 2** and Appendix A **Fig. S2**), with the highest values usually observed in Area-I. In most of the time, DO concentrations increased in the order: Area-*I* < Area-III < Area-II < Area-IV. However, in March, DO concentrations in Area-II were higher than those in other three areas (**Table 2** and Appendix A **Fig. S2**).

Table 2

Summary of the two-way ANOVA results determining the effect of sampling water areas, seasons, and their interactions on water environmental variables in Wenwusha Reservoir

	df	pH	DO	TOC	NH_4^+	TDN	PO_4^{3-}
Sampling area	3	17.00**	201.52**	1078.99**	22.02**	85.31**	7.368**
Season	2	1046.31**	1046.16**	2.37	32.65**	19.91**	14.953**
Sampling area × Season	6	11.64**	115.55**	4.78**	1.14	29.72**	9.012**

Symbols * and ** indicate significant differences at 0.05 and 0.01, respectively.

In general, sampling sites around human-dominated landscapes (residential area, aquaculture pond, and farmland) in NRA in the Wenwusha reservoir had higher nutrient levels (i.e. TOC, TDN, and NH_4^+ concentration), pH value and Chl-*a* concentrations but lower DO concentrations than those near the natural landscapes, such as wetland and forest in SRA.

2.2. Spatial variation in CO_2 dynamics across four water areas

During the sampling period, large spatial variations in CO_2 concentrations were observed across different areas. Dissolved CO_2 concentrations in Area-I, Area-II, Area-III, and Area IV varied over the ranges of 1.80–178.26 µmol/L, 0.07–239.74 µmol/L, 3.21–59.17 µmol/L, and 1.02–64.91 µmol/L, respectively. Dissolved CO_2 concentrations decreased significantly in the order: Area-I (52.89 ± 3.64 µmol/L) > Area-II (49.22 ± 2.95 µmol/L) > Area-III (29.51 ± 2.88 µmol/L) > Area-IV (22.03 ± 1.53 µmol/L) ($p < 0.001$, **Fig. 2** and **Fig. 4a**).

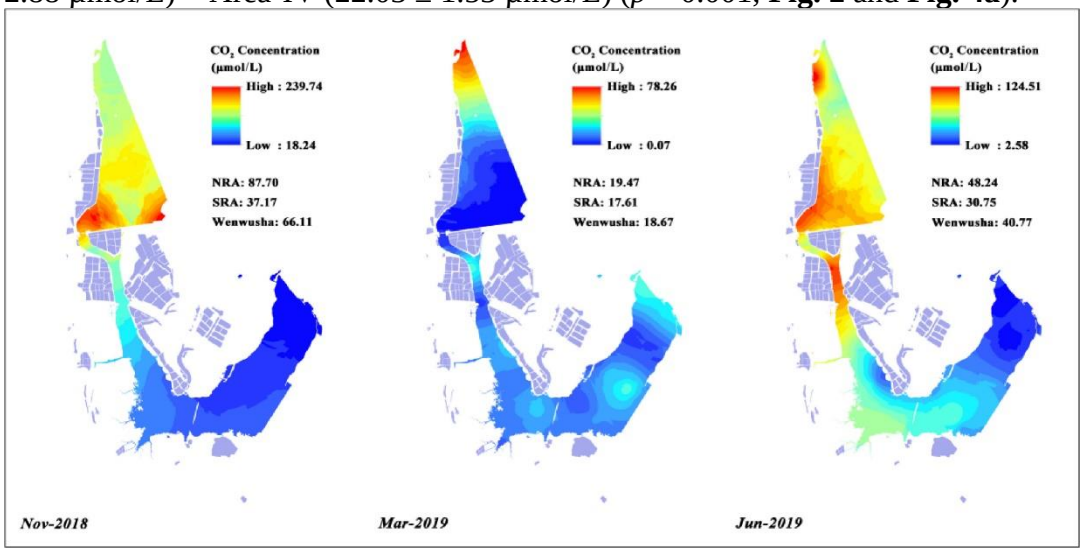

Fig. 2. Spatial distribution of dissolved CO_2 concentrations in surface water (~0.2 m depth) of Wenwusha Reservoir from November 2018 to June 2019.

Across the three sampling campaigns, CO_2 fluxes across the water-air interface decreased in the order: Area-I (5.05 ± 0.87 mmol/m^2/hr) > Area-II (2.22 ± 0.27 mmol/m^2/hr) > Area-IV (1.62 ± 0.33 mmol/m^2/hr) > Area-III (1.46 ± 0.34 mmol/m^2/hr) (**Fig. 3** and **Fig. 4b**). With the exception of March 2019, mean CO_2 fluxes across the water-air interface show large differences among the four water areas ($p < 0.05$, **Fig. 4b**).

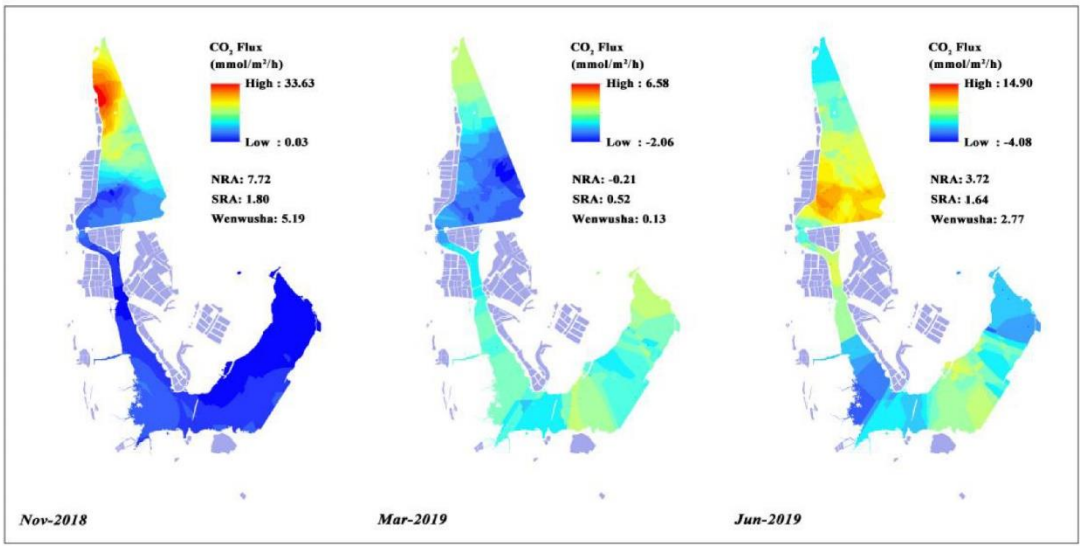

Fig. 3. Spatial distribution of CO_2 fluxes across the water-air interface in Wenwusha Reservoir from November 2018 to June 2019.

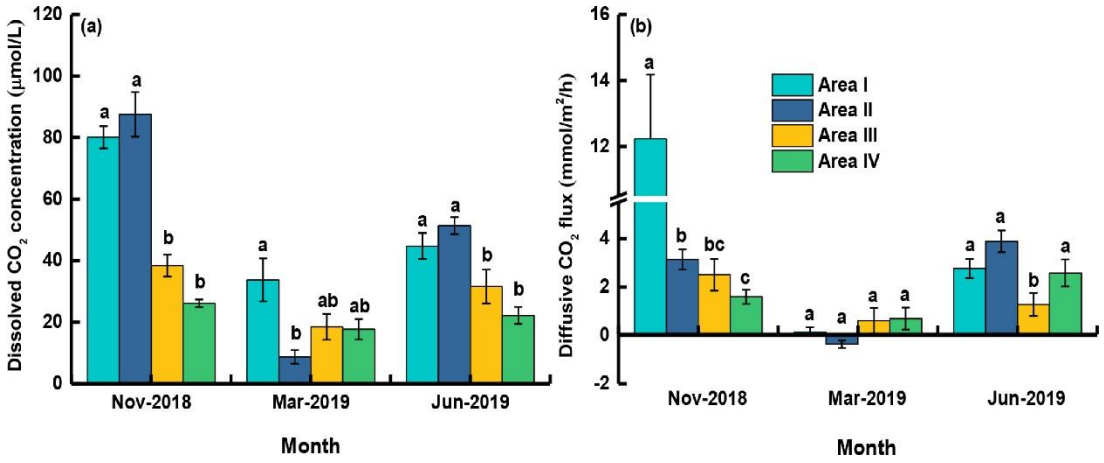

Fig. 4. Variations in mean CO_2 concentrations (a) and fluxes (b) among the four water areas in Wenwusha Reservoir from November 2018 to June 2019. Different letters denote significant differences across water areas (p<0.05) based on the results of one-way ANOVA. Area I, mainly surrounded by urban land (n = 28); Area II, mainly surrounded by agricultural land (n = 40); Area III, mainly surrounded by wetland and sporadic agricultural land (n = 12); Area IV, mainly surrounded by forest and sand (n = 22). Data were shown with mean ± SE.

2.3. Spatial variation in CO_2 dynamics between two reservoir areas

Significant spatial differences of CO_2 dynamics were also observed between NRA and SRA. Mean CO_2 concentration and flux in NRA (51.32 ± 3.19 μmol/L and 3.72 ± 0.47 mmol/m²/hr) were significantly higher than those in SRA (29.71 ± 1.87 μmol/L and 1.64 ± 0.22 mmol/m²/hr) (p < 0.01, Appendix A **Fig. S3**). Larger CO_2 concentration and emission were often obtained in the water areas with higher urbanization level around, mainly in NRA (**Fig. 2** and **Fig. 3**).

2.4. Spatial variation in CO_2 dynamics between different microtopographic zones

CO_2 concentration and flux were compared between different microtopographic zones (Appendix A **Fig. S4**). The mean dissolved CO_2 concentration in narrow waters (52.25 ± 4.62 μmol/L) was significantly higher than that in the open waters (37.58 ± 2.09 μmol/L) ($p < 0.05$, Appendix A **Fig. S4a**). No significant difference in mean dissolved CO_2 concentration was found between the shallow water zone and deep water zone (41.51 ± 3.09 and 42.09 ± 2.68 μmol/L, respectively, $p > 0.05$, Appendix A **Fig. S4b**). The mean CO_2 fluxes across the water-air interface in the narrow and open waters were 2.63 ± 0.50 mmol/m²/hr and 2.83 ± 0.34 mmol/m²/hr, respectively. The mean CO_2 fluxes in the shallow water zone and deep water zone were 2.33 ± 0.37 mmol/m²/hr and 3.07 ± 0.40 mmol/m²/hr, respectively (Appendix A **Fig. S4c** and **Fig. S4d**). All sampling sites showed no significant spatial differences of mean CO_2 flux between different reservoir microtopographic zones ($p > 0.05$, Appendix A **Fig. S4**).

2.5. Temporal variation in CO_2 concentration and flux

There were clear seasonal variations in dissolved CO_2 concentration throughout the reservoir (**Fig. 2**), with the highest concentration in Nov-2018 (66.11 ± 3.97 μmol/L), followed by Jun-2019 (40.77 ± 2.11 μmol/L) and Mar-2019 (18.67 ± 2.44 μmol/L). CO_2 undersaturation of water samples (i.e. saturation < 100%) were found in Mar-2019 and Jun-2019 (**Fig. 2**). There were also seasonal variations in CO_2 fluxes across the water-air interface. CO_2 fluxes during the whole period ranged from −4.09 to 33.63 mmol/m²/hr. More than half of the measurements made in the spring (Mar-2019) exhibited net CO_2 uptake (**Fig. 3**). Seasonal mean CO_2 fluxes were 5.19 ± 0.70 mmol/m²/hr in Nov-2018, 0.13 ± 0.15 mmol/m²/hr in Mar-2019, and 2.99 ± 0.29 mmol/m²/hr in Jun-2019, respectively. The four water areas showed similar seasonal patterns of CO_2 concentrations and fluxes: Mar-2019 < Jun-2019 < Nov-2018 ($p < 0.001$, **Figs. 2–4**).

2.6. Relationship between CO_2 concentration / flux and water physio-chemical properties

Spearman correlations were conducted to examine the relationships between CO_2 concentration (or flux) with the physio-chemical properties of water (**Fig. 5, 6** and **Table 3**). Dissolved CO_2 concentrations were positively correlated with pH, NH_4^+, TDN and TOC, but negatively correlated with water temperature and DO ($p < 0.01$, **Table 3**). CO_2 fluxes were positively correlated with TOC and NH_4^+, but negatively correlated with DO ($p < 0.05$, **Table 3**). Notably, the significance and strength of correlations were different among four water areas. CO_2 concentrations and fluxes were significantly and negatively correlated with DO concentrations in three water areas except Area-III (**Fig. 5a** and **6a**). CO_2 concentrations were positively correlated with NH_4^+ and TOC concentrations, with stronger relationships found in Area-I and Area-II (**Fig. 5b** and **5c**).

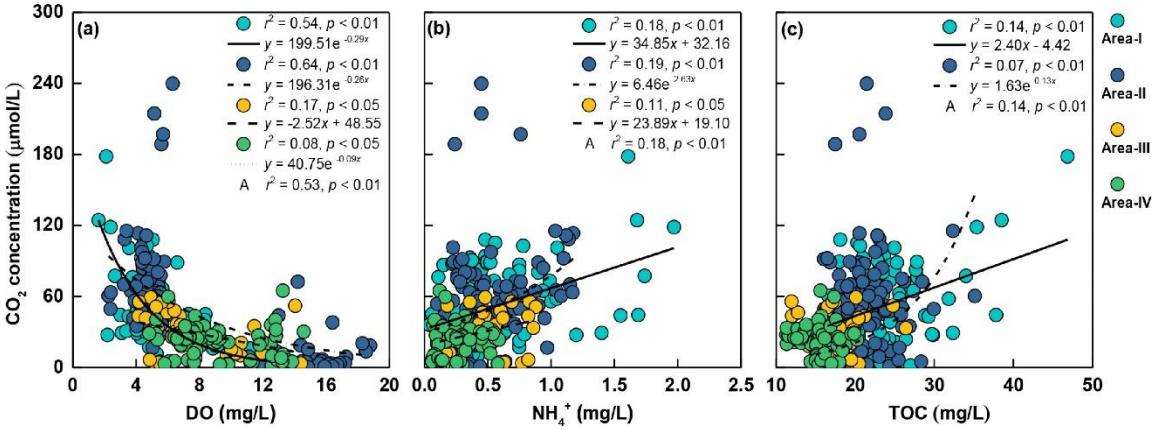

315

316 Fig. 5. Relationships of CO_2 concentration against DO (a), NH_4^+ (b), and TOC (c) in the four
317 water areas. Letter A in the legend denotes all water areas combined.

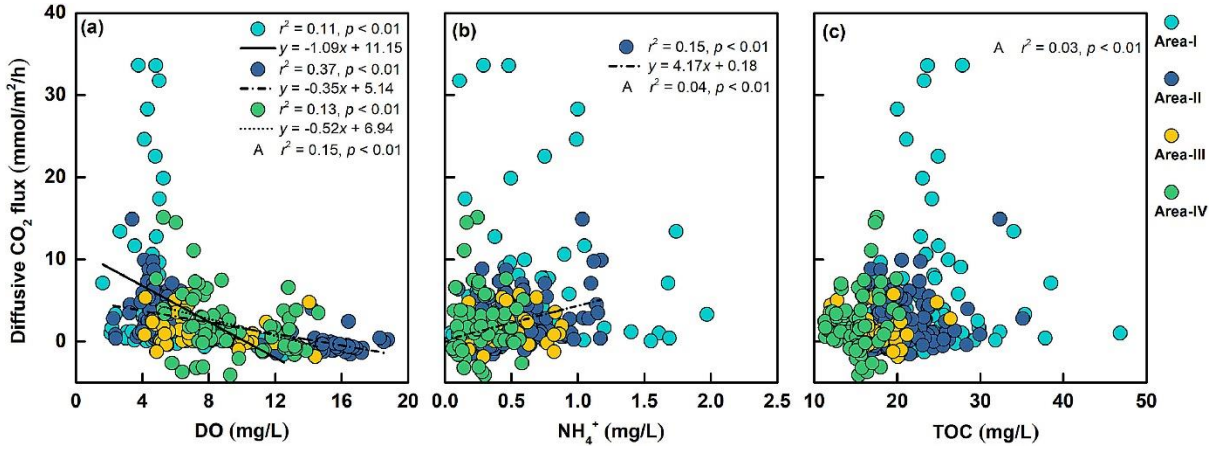

318

319 Fig. 6. Relationships of CO_2 flux against DO (a), NH_4^+ (b), and TOC (c) in the four water
320 areas. Letter A in the legend denotes all water areas combined.

321

322

Table 3

Spearman correlation coefficients of CO_2 concentration (flux) with environmental variables in the whole Wenwusha Reservoir during the research period.

Environmental variables	CO_2 concentration	CO_2 flux
Water temperature (Tw)	-0.226**	NS
pH	0.195**	NS
Dissolved oxygen (DO)	-0.732**	-0.573**
Total organic carbon (TOC)	0.381**	0.137*
Ammonia (NH_4^+)	0.471**	0.323**
Total dissolved nitrogen (TDN)	0.151**	NS
Phosphate (PO_4^{3-})	NS	NS

NS means "nonsignificant correlation". Symbols * and ** indicate significant correlations at 0.05 and 0.01 levels, respectively.

Redundancy analysis (RDA) was performed for the two reservoir areas, NRA and SRA, with CO_2 concentration and flux as the response variables and water physio-chemical properties as the explanatory variables. In NRA, axis I explained 55.1% of the variations in CO_2 concentration and flux, with DO and TOC being the most powerful predictors (**Fig. 7**). In SRA, axis I explained 44.9% of the variations in CO_2 concentration and flux, with NH_4^+, DO, and TOC being the major controlling factors (**Fig. 7**).

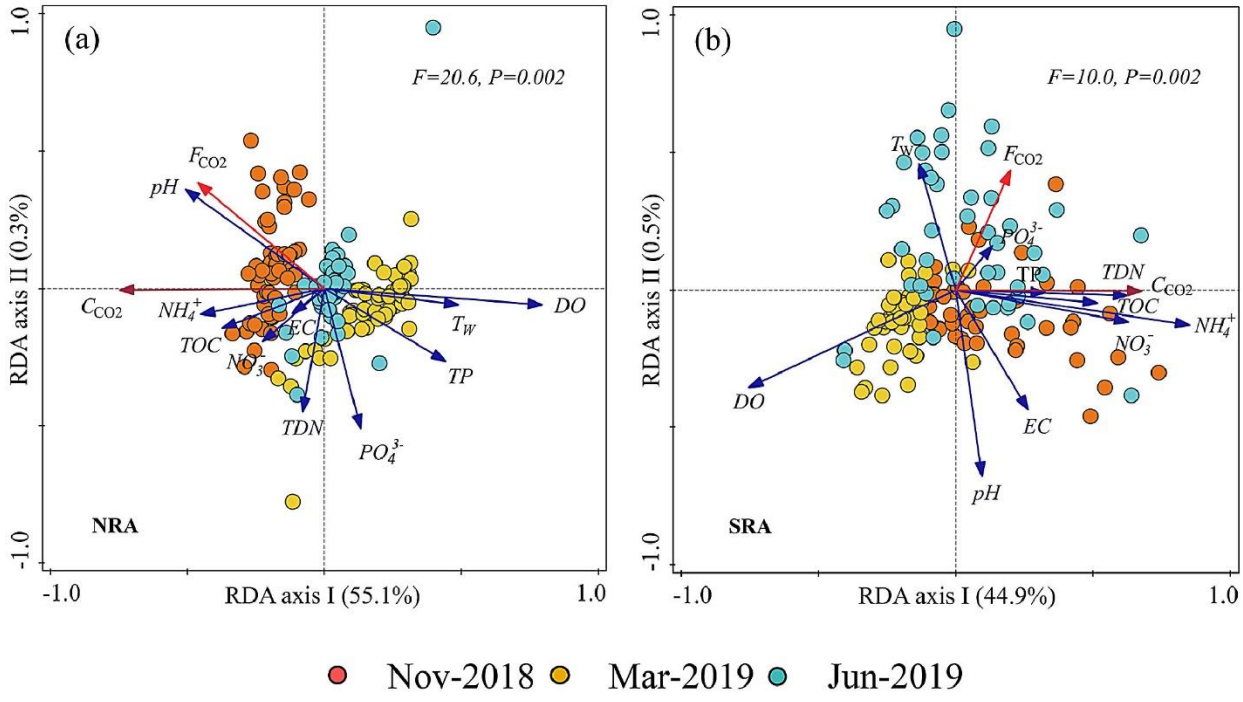

Fig. 7. Results of redundancy analysis (RDA) showing the relations between CO_2 concentration (or CO_2 flux) and water physico-chemical properties including T_W (water temperature), pH, *EC* (conductivity), *DO* (dissolved oxygen), NO_3^- (nitrate nitrogen), NH_4^+ (ammonia nitrogen), PO_4^{3-} (phosphate), and *TP* (total phosphorus), in the north reservoir area (NRA) (a) and the south reservoir area (SRA) (b) in Wenwusha Reservoir.

3. Discussion

3.1. Effects of watershed urbanization and land use types on CO_2 dynamics

Land use change in the catchment can disturb the biogeochemical cycling on land and in adjacent waters (Lai et al., 2016; Zhang et al., 2015), resulting in large spatial variations in CO_2 fluxes (Kamjunke et al., 2013; Pacheco et al., 2015). In our study, the concentrations of carbon and nitrogen substrates (TOC, $NH_4^+$and TDN) in Area-III and Area-IV were substantially lower than those in Area-I and Area-II where waters were close to municipal and agricultural lands (**Table 2** and Appendix A **Fig. S3**). The CO_2 concentrations and fluxes increased with TOC and NH_4^+ concentrations across the whole reservoir ($p < 0.05$, **Table 3**). Our results revealed that the spatial variation in CO_2 flux in the subtropical Wenwusha reservoir was affected by anthropogenic activities (e.g., urbanization and land use change) in the catchment, which were similar to previous findings (Marescaux et al., 2018; Wang et al., 2017) that CO_2 production and emission in the waters increased with the levels of urbanization and sewage discharge. Two underlying processes may account for this: (1) the large TOC load from municipal and aquaculture effluents provides more substrates for *in situ* heterotrophic respiration (Almeida et al., 2016; Crawford et al., 2013); (2) additional nitrogen loading in water areas with high organic carbon concentrations (e.g. Area I) can

ameliorate nitrogen limitation on microbial decomposition and promote net CO_2 production (Bodmer et al., 2016; Marescaux et al., 2018;).

The highest mean CO_2 flux observed in Area-I provided additional evidence for the impact of urbanization on CO_2 emission from our reservoir. In general, urban and agricultural sewage carries abundant dissolved CO_2 (Webb et al., 2016; Yang et al., 2018; Yu et al., 2017). The spatial variation in reservoir CO_2 flux adjacent to urban areas is thus often affected by sewage discharge. In this study, we observed that the dissolved CO_2 concentrations in the sewage drainage channels, aquaculture ponds, and rivers adjacent to the reservoir were about three times higher than those in the reservoir surface water. This resulted in the direct input of dissolved CO_2 into the Wenwusha Reservoir, and subsequently a larger CO_2 diffusive flux because of the steeper CO_2 concentration gradient between the surface water and the atmosphere. Therefore, the discharge of CO_2-rich wastewater can directly contribute to CO_2 oversaturation in some polluted waters and lead to high CO_2 emissions from reservoir water to the atmosphere (Li et al., 2020a; 2020b).

Topography can also influence the transport and distribution of pollutants. Pollutants tend to accumulate in the narrow coastal waters due to their low water exchange and dilution effect (e.g. Arneth et al., 2017; Li et al., 2013; Ni et al., 2019). For instance, Natchimuthu et al. (2017) reported that small and narrow lakes had higher pCO_2 and CO_2 fluxes in a Swedish catchment. Similar observations have been found in other aquatic ecosystems with varying microtopography (Raymond and Cole, 2003; Schilder et al., 2013; Wang et al., 2017). Across the entire Wenwusha Reservoir, the mean CO_2 concentrations and fluxes from the shallow water zone to deep water zone showed no significant difference ($p > 0.05$, Appendix A **Fig S4c** and **S4d**). The reservoir was shallow, with mean and maximum depths of 1.5 and 4.0 m, respectively. The reservoir bottom was quite flat with little variations in sediment-to-water volume ratio among reservoir areas (Gruber et al., 2019; Roland et al., 2010; Wilson et al., 2015), which resulted in limited effects of depth on DOC concentration and sediment respiration. Moreover, CO_2 concentrations increased significantly from the open water areas to the narrow areas ($p < 0.05$, Appendix A **Fig S4a**), which might be related to the coupling of high pollution load and topography (Kortelainen et al., 2006; Roland et al., 2010; Zhang et al., 2019). On one hand, narrow waters have relatively lower velocity and a more enclosed environment than other parts of the reservoir (Holgerson, 2015; Xiao et al., 2017), providing favorable conditions for the accumulation of fresh sediments and thus respiratory CO_2 production. On the other hand, the narrow waters adjacent to aquaculture ponds and ditches can receive abundant non-point source sewage. Similar to the spatial patterns of CO_2 concentration, TOC, NH_4^+, and TDN concentrations at the narrow waters were approximately 28%, 100%, and 27% larger than those at the open areas, which supported the above hypothesis.

3.2. Temporal variation in CO_2 emission

During the study period, mean CO_2 concentrations in Wenwusha Reservoir exhibited prominent seasonal fluctuations with higher value in autumn (Nov-2018) and lower value in spring (Mar-2019) (**Fig. 4a**). Correspondingly, CO_2 flux followed the same temporal pattern (**Fig. 4b**). In general, net CO_2 flux (release / uptake) in aquatic ecosystems reflects the balance between CO_2 production and consumption (Jonsson et al., 2003; Bellido et al., 2009; Pacheco et al., 2015). Some researches attributed the variability of CO_2 flux to organic matter decomposition (Wang et al., 2017), primary productivity (Sobek et al., 2005), and meteorological conditions (Butman and Raymond, 2011; Natchimuthu et al., 2014).

Biodegradation of organic carbon is regarded as an important source of CO_2 production (Barros et al., 2011; Crawford et al., 2013; Demarty et al., 2009). However, our

measurements showed no significant seasonal change in TOC (**Table 2**), which was different from the temporal patterns of CO_2 concentrations and fluxes in the reservoir. Therefore, substrate supply was likely not a key factor affecting the temporal dynamics of CO_2 in Wenwusha Reservoir. Algal photosynthesis consumes CO_2, which can play an important role in governing the temporal variation in CO_2 flux (Kutzbach et al., 2007; Scofield et al., 2016; Yao et al., 2007). Chl-*a* is an important parameter characterizing algal primary production. Despite the lack of significant correlation observed between Chl-*a* and CO_2 flux in the current research, the seasonal pattern of mean water Chl-*a* concentration was opposite to that of CO_2 (**Fig. 4** and Appendix A **Fig. S5**). Limited by the low temperature, relatively lower Chl-*a* concentration and the highest CO_2 emissions were seen in November 2018. Higher Chl-*a* concentration coincided with rising temperature in spring, accounting for the lower CO_2 concentration and flux in March 2019 (Appendix A **Fig. S5**). It should be noted that precipitation and its dilution effect on Chl-*a* in water could also influence the seasonal variation in CO_2 flux (Holgerson, 2015; Zhang et al., 2019). In addition, on rainy days, photosynthesis could be constrained by lower solar radiation. Frequent rainfall events between April and June 2019 (total precipitation of 625.6 mm) (Appendix A **Fig. S1**) reduced Chl-*a* concentration in the reservoir to some extent. Thus, the higher CO_2 flux detected in summer (June-2019) than in spring (Mar-2019) was probably in part due to the greater number of rainy days and the subsequent decline of sunlight-driven photosynthesis. In the subtropical coastal reservoir, therefore, our findings demonstrated that primary productivity could exert an impact on the seasonal variation in CO_2 fluxes between seasons, which in turn would be related to precipitation and temperature.

3.3. CO_2 fluxes in comparison with previous estimates

The average CO_2 flux from Wenwusha Reservoir was 2.77 ± 0.28 mmol/m^2/h, which was lower than those reported in some tropical waters (e.g. Abril et al., 2005; Dos Santos et al., 2006; Guérin et al., 2006) (**Table 4**). However, we noticed that the CO_2 fluxes from our reservoir were markedly higher than those in most temperate and subtropical reservoirs worldwide, such as Lake Lynch in Chile (Gerardo-Nieto et al., 2017), Eagle Creek reservoir in the USA (Jacinthe et al., 2012), cascade reservoirs on Maotiao river in China (Wang et al., 2011), and Danjiangkou reservoir in China (Li and Zhang, 2014) (**Table 4**). Our results of flux upscaling to the whole-reservoir scale based on our high spatial resolution data showed that Wenwusha reservoir emitted approximately 3.91 Gg CO_2 per year. The total CO_2 flux from Wenwusha reservoir would hence account for approximately 0.0241% of the annual total from all the reservoirs in China (Li et al., 2018). The results of this study showed that the subtropical coastal reservoir such as Wenwusha reservoir could be potential sources of atmospheric CO_2 and therefore would deserve more attention.

Table 4

Ranges of CO_2 fluxes (mmol m^{-2} h^{-1}) from different types of reservoirs in the world.

Climate	Site	Main land use in the catchment	F_{CO2} (mmol m^{-2} h^{-1})	Reference
Temperate	Lake Lynch, Chile	Forest	0.49 – 0.57 (0.52)	Gerardo-Nieto et al., 2017
	L.Skinnmuddselet, Sweden	Forest, mire	------- (0.83)	Åberg et al., 2004
	Porttipahta, Finland	Forest, pond	0.83 – 2.17 (1.46)	Huttunen et al., 2003
	Lokka, Finland	Peatland	0.46 – 3.04 (1.44)	Huttunen et al., 2003
	Eagle Creek, USA	Agriculture, grassland, forest	-1.28 – 15.10 (1.90)	Jacinthe et al., 2012
Subtropical	Danjiangkou, China	Forest, grassland, farmland	-0.34 – 1.31 (0.38)	Li & Zhang, 2014
	Xiuwen, China	-------	-0.25 – 3.71 (1.96)	Wang et al., 2011
	Chongqing, China	Urban	-0.42 – 21.25 (5.73)	Wang et al., 2017
	Chongqing, China	Agriculture	-0.48 – 7.20 (2.01)	Wang et al., 2017
	Al-Wihdeh, King Talal, Wadi , Al-Arab, Jordan	-------	-1.10 – 16.52 (3.12)	Alshboul et al., 2015
	Wenwusha, China	Urban, agriculture, forest, wetland	-4.09 – 33.63 (2.77)	This study
Tropical	Petit Saut, French Guiana	Tropical forest	-0.42 – 15.42 (5.54)	Abril et al., 2005
	Tucurui, Brazil	Tropical forest	------- (7.92)	Dos Santos et al., 2006
	Samuel, Balbina, Brazil	Tropical forest	10.58 – 16.33	Guerin et al., 2006
	Cerrado, Brazil	-------	-0.34 – 16.62	Roland et al., 2011
-------	China's reservoirs	-------	------- (1.85)	Li et al., 2018
	Global reservoirs	-------	------- (1.14)	Deemer et al., 2016

Figures in brackets are averages. "-------" means no data.

Notably, the average CO_2 flux in waters adjacent to the urban area (Area-I, 5.05 ± 0.87 mmol/m^2/hr) was 1.72 − 3.46 times of that in other water areas in Wenwusha Reservoir (**Fig. 3** and **Fig. 4b**). Moreover, the mean CO_2 flux in Area-I was close to the level seen in some tropical reservoirs (Barros et al., 2011) and urban reservoirs in Chongqing, Southwest China (5.73 ± 3.38 mmol/m^2/hr) (Wang et al., 2017), where urban pollution was the major contributor to CO_2 production. In contrast with the findings from several reservoirs in Chongqing (Wang et al., 2017), our results showed that the influence of urbanization on CO_2 emission from adjacent waters could also exist in different areas within a single reservoir ecosystem. These results together indicated the crucial role of urbanization in carbon biogeochemical cycling in reservoir waters.

3.4. Uncertainties and further outlook

There are several limitations in our study that are worthy addressing. Firstly, our results have shown large spatiotemporal variations in CO_2 concentration and flux in the reservoir. In future studies, field sampling with a greater frequency over multiple years can provide more detailed information about the temporal variations in CO_2 dynamics at multiple scales. Secondly, the diel fluctuations of GHG flux have been reported in various aquatic ecosystems (Natchimuthu et al., 2014; Xiao et al., 2013; Xing et al., 2004). Photosynthesis is typically strong during the day, while respiration dominates CO_2 exchange with markedly higher CO_2 emission at night (Hirota et al., 2007). Therefore, aquatic ecosystems can be a net carbon sink during the daytime due to the strong phytoplankton photosynthesis, but change to a net carbon source when considering a complete 24-hour cycle owing to the strong carbon emission at night (Natchimuthu et al., 2014). Similar diel patterns can also occur in the reservoir on top of the seasonal variation. A greater number of *in situ* measurement of the diurnal CO_2 fluxes in different seasons will further improve our development of annual CO_2 budgets in the aquatic ecosystems. Furthermore, some studies have shown the important role of meteorological variables in affecting CO_2 emission (Li and Lu, 2012; Natchimuthu et al., 2014; Zhao et al., 2013). Although the effect of extreme weather events, such as heavy rain and typhoon, on CO_2 flux was not examined in this study, we found some clear impacts of continuous precipitation on reservoir CO_2 fluxes. The impacts of meteorological events deserve more attention in future studies. Due to the limitation of equipment, we did not measure sewage discharge and nutrient concentrations in this study. In future work, quantifying the rates of water and nutrient inputs from sewage can provide useful information to improve the understanding of the impact of urbanization and land use on carbon cycling in reservoirs. Lastly, we focused our investigation of the controls of CO_2 concentration and flux on various environmental parameters (e.g. water quality, weather condition, and reservoir morphology). Future research can quantify the biogeochemical processes of CO_2 using molecular biotechnology and isotope methods to yield a better mechanistic understanding of the spatiotemporal dynamics of CO_2 in aquatic ecosystems.

4. Conclusions

With the worsening climate change, GHG emission from reservoirs have received increasing attention. In this study, dissolved CO_2 concentration and flux were investigated at high spatial resolution from a subtropical coastal Wenwusha Reservoir, Southeast China. Overall, our results showed that CO_2 concentrations in the reservoir were supersaturated (average: 24.25 mol/m^2/y) in most periods, varying over a wide range from −35.82 to 294.60 mol/m^2/y. CO_2 concentrations and fluxes from waters adjacent to regions with intensive human activity were much higher than those in other areas, due to larger input of allochthonous carbon and nitrogen via municipal sewage, aquaculture wastewater and upstream runoff. Urbanization

and agricultural activities in the catchment appeared to create CO_2 emission hotspots in some parts of the reservoir. Apart from the spatial differences across the reservoir, reservoir CO_2 emissions also exhibited clear seasonal variations that were related to primary productivity, temperature, and rainfall events. Our results highlighted that subtropical coastal reservoir was a net source of atmospheric CO_2 with high spatiotemporal heterogeneity. Considering the rapid urbanization in coastal areas around the world, proactive measures are needed to mitigate the large GHG emission from coastal reservoirs arising from human activities.

Acknowledgment

This research was supported by the National Science Foundation of China (Nos. 41801070, 41671088), the National Science Foundation of Fujian Province (No. 2020J01136), 2020 Innovation Training Programme Project for Fujian Normal University Student's (No. cxxl-2020270), the Research Grants Council of the Hong Kong Special Administrative Region, China (Nos. CUHK458913, 14302014, 14305515), the CUHK Direct Grant (No. SS15481), Open Research Fund Program of Jiangsu Key Laboratory of Atmospheric Environment Monitoring and Pollution Control (No. KHK1806), a project funded by the Priority Academic Program Development of Jiangsu Higher Education Institutions (PAPD) and the Minjiang Scholar Programme.

References

Åberg, J., Bergström, A.K., Algesten, G., Söderback, K., Jansson, M., 2004. A comparison of the carbon balances of a natural lake (L.Örträsket) and a hydroelectric reservoir (L.Skinnmuddselet) in northern Sweden. Water Res. 38, 531–538. https://doi.org/10.1016/j.watres.2003.10.035.

Abril, G., Guerin, F., Richard, S., Delmas, R., Galy-Lacaux, C., Gosse, P., Tremblay, A., Varfalvy, L., Dos Santos, M.A., Matvienko, B., 2005. Carbon dioxide and methane emissions and the carbon budget of a 10-year old tropical reservoir (Petit Saut, French Guiana). Glob. Biogeochem. Cycles 19. https://doi.org/10.1029/2005GB002457.

Almeida, R.M., Paranaíba J.R., Barbosa Í., Sobek S., Kosten S., Linkhorst A., Mendonça R., Quadra G., Roland F., Barros N., 2019. Carbon dioxide emission from drawdown areas of a Brazilian reservoir is linked to surrounding land cover. Aquatic. Ences. 81, 1–9. https://doi.org/10.1007/s00027-019-0665-9.

Almeida, R.M., Nóbrega, G.N., Junger, P.C., Figueiredo, A.V., Andrade, A.S., de Moura, C.G.B., Tonetta, D., Oliveira, E.S., Araújo, F., Rust, F., Piñeiro-Guerra, J.M., Mendonça, J.R., Medeiros, L.R., Pinheiro, L., Miranda, M., Costa, M.R.A., Melo, M.L., Nobre, R.L.G., Benevides, T., Roland, F., De Klein, J., Barros, N.O., Mendonça, R., Becker, V., Huszar, V.L.M., Kosten, S., 2016. High primary production contrasts with intense carbon emission in a eutrophic tropical reservoir. Front. Microbiol. 7, 717. https://doi.org/10.3389/fmicb.2016.00717.

Alshboul, Z., Lorke, A., 2015. Carbon dioxide emissions from reservoirs in the lower Jordan watershed. Plos One 10. https://doi.org/10.1371/journal.pone.0143381.

Arneth, A., Sitch, S., Pongratz, J., Stocker, B.D., Ciais, P., Poulter, B., Bayer, A.D., Bondeau, A., Calle, L., Chini, L.P., Gasser, T., Fader, M., Friedlingstein, P., Kato, E., Li, W., Lindeskog, M., Nabel, J.E.M.S., Pugh, T.A.M., Robertson, E., Viovy, N., Yue, C., Zaehle, S., 2017. Historical carbon dioxide emissions caused by land-use changes are possibly larger than assumed. Nat. Geosci. 10, 79. https://doi.org/10.1038/ngeo2882.

539 Barros, N., Cole, J.J., Tranvik, L.J., Prairie, Y.T., Bastviken, D., Huszar, V.L.M., Del
540 Giorgio, P., Roland, F., 2011. Carbon emission from hydroelectric reservoirs linked to
541 reservoir age and latitude. Nat. Geosci. 4, 593–596. https://doi.org/10.1038/ngeo1211.

542 Bellido, J.L., Tulonen, T., Kankaala, P., Ojala, A., 2009. CO_2 and CH_4 fluxes during spring
543 and autumn mixing periods in a boreal lake (paajarvi, southern finland). J. Geophys. Res-
544 Biogeosci. 114. https://doi.org/10.1029/2009jg000923.

545 Bevelhimer, M.S., Stewart, A.J., Fortner, A.M., Phillips, J.R., Mosher, J.J., 2016. CO_2 is
546 dominant greenhouse gas emitted from six hydropower reservoirs in southeastern United
547 States during peak summer emissions. Water 8, 1–14. http://doi.org/10.3390/ w8010015.

548 Bodmer, P., Heinz, M., Pusch, M., Singer, G., Premke, K., 2016. Carbon dynamics and their
549 link to dissolved organic matter quality across contrasting stream ecosystems. Sci. Total
550 Environ. 553, 574–586. http://doi.org/10.1016/j.scitotenv.2016.02.095.

551 Butman, D., Raymond, P.A., 2011. Significant efflux of carbon dioxide from streams and
552 rivers in the united states. Nat. Geosci. 4, 839–842. http://doi.org/10.1038/ngeo1294.

553 Chao, B.F., Wu, Y.H., Li, Y.S., 2008. Impact of artificial reservoir water impoundment on
554 global sea level. Science 320, 212–214. http://doi.org/10.1126/science.1154580.

555 Cole, J.J., Bade, D.L., Bastviken, D., Pace, M.L., Van De Bogert, M., 2010. Multiple
556 approaches to estimating air-water gas exchange in small lakes. Limnol. Oceanogr-Meth.
557 8, 285–293. http://doi.org/10.4319/lom.2010.8.285.

558 Crawford, J.T., Striegl, R.G., Wickland, K.P., Dornblaser, M.M., Stanley, E.H., 2013.
559 Emissions of carbon dioxide and methane from a headwater stream network of interior
560 alaska. J. Geophys. Res-Biogeosci. 118, 482–494. http://doi.org/10.1002/jgrg.20034.

561 Crusius, J., Wanninkhof, R., 2003. Gas transfer velocities measured at low wind speed over a
562 lake. Limnol. Oceanogr. 48, 1010–1017. http://doi.org/10.4319/lo.2003.48.3.1010.

563 Deemer, B.R., Harrison, J.A., Li, S.Y., Beaulieu, J.J., Delsontro, T., Barros, N., Bezerra-
564 Neto, J.F., Powers, S.M., Santos, M.A.D., Vonk, J.A., 2016. Greenhouse gas emissions
565 from reservoir water surfaces: a new global synthesis. Bioscience 66, 949−964.
566 https://doi.org/10.1093/biosci/biw117.

567 Demarty, M., Bastien, J., Tremblay, A., Hesslein, R.H., Gill, R., 2009. Greenhouse gas
568 emissions from boreal reservoirs in manitoba and quebec, canada, measured with
569 automated systems. Environ. Sci. Technol. 43, 8908–8915. http://doi.org/10.1021/
570 es8035658.

571 De Mello, K., Valente, R.A., Randhir, T.O., Alves Dos Santos, A.C., Vettorazzi, C.A., 2018.
572 Effects of land use and land cover on water quality of low-order streams in southeastern
573 brazil: Watershed versus riparian zone. Catena 167, 130–138. http://doi.org/
574 10.1016/j.catena.2018.04.027.

575 Dodds, W.K., Cole, J.J., 2007. Expanding the concept of trophic state in aquatic ecosystems:
576 It's not just the autotrophs. Aquat. Sci. 69, 427–439. http://doi.org/10.1007/ s00027-007-
577 0922-1.

578 Dos Santos, M.A., Rosa, L.P., Sikar, B., Sikar, E., Dos Santos, E.O., 2006. Gross greenhouse
579 gas fluxes from hydro-power reservoir compared to thermo-power plants. Energ. Policy
580 34, 481–488. http://doi.org/10.1016/j.enpol.2004.06.015.

581 Domingues R.B., Catia G.C., Galvao H.M., Brotas V., Barbosa A.B., 2016. Short-term
582 interactive effects of ultraviolet radiation, carbon dioxide and nutrient enrichment on

583 phytoplankton in a shallow coastal lagoon. Aquat. Ecol. 51, 91–105.
584 http://doi.org/10.1007/s10452-016-9601-4.

585 Fearnside P.M., 2005. Brazil's Samuel dam: Lessons for hydroelectric development policy
586 and the environment in Amazonia. Environ. Manage. 2005, 399, 1–19. http://doi.org/
587 10.1007/s00267-004-0100-3.

588 Fuzhou Municipal Water Authorities, 2019. Water Resources Bulletin in 2018.
589 http://slj.fuzhou.gov.cn/zz/zyxz/201912/t20191205_3109364.htm.pdf (In Chinese).

590 Gerardo-Nieto, O., Soledad Astorga-Espana, M., Mansilla, A., Thalasso, F., 2017. Initial
591 report on methane and carbon dioxide emission dynamics from sub-antarctic freshwater
592 ecosystems: A seasonal study of a lake and a reservoir. Sci. Total Environ. 593, 144–154.
593 http://doi.org/10.1016/j.scitotenv.2017.02.144.

594 Gruber, N., Clement, D., Carter, B.R., Feely, R.A., Van Heuven, S., Hoppema, M., Ishii, M.,
595 Key, R.M., Kozyr, A., Lauvset, S.K., Lo Monaco, C., Mathis, J.T., Murata, A., Olsen, A.,
596 Perez, F.F., Sabine, C.L., Tanhua, T., Wanninkhof, R., 2019. The oceanic sink for
597 anthropogenic CO_2 from 1994 to 2007. Science 363, 1193. http://doi.org/
598 10.1126/science.aau5153.

599 Guérin, F., Abril, G., Richard, S., Burban, B., Reynouard, C., Seyler, P., Delmas, R., 2006.
600 Methane and carbon dioxide emissions from tropical reservoirs: significance of
601 downstream rivers. Geophys. Res. Lett. 33, L21407. http://doi.org/10.1029/
602 2006GL027929.

603 Guérin, F., Abril, G., Serca, D., Delon, C., Richard, S., Delmas, R., Tremblay, A., Varfalvy,
604 L., 2007. Gas transfer velocities of CO_2 and CH_4 in a tropical reservoir and its river
605 downstream. J. Mar. Syst. 66, 161–172. https://doi.org/10.1016/j.jmarsys.2006.03.019.

606 Hao, B.F., Ma, M.G., Li, S.W., Li, Q.P., Hao, D.L., Huang, J., Ge, Z.X., Yang, H., Han, X.J.,
607 2019. Land Use Change and Climate Variation in the Three Gorges Reservoir Catchment
608 from 2000 to 2015 Based on the Google Earth Engine. Sensors 19(9). https://doi.org/
609 10.3390/s19092118.

610 Hertwich, E.G., 2013. Addressing biogenic greenhouse gas emissions from hydropower in
611 LCA. Environ. Sci. Technol. 47, 9604−9611. https://doi.org/10.1021/es401820p.

612 Hirota, M., Senga, Y., Seike, Y., Nohara, S., Kunii, H., 2007. Fluxes of carbon dioxide,
613 methane and nitrous oxide in two contrastive fringing zones of coastal lagoon, Lake
614 Nakaumi, Japan. Chemosphere 68, 597–603. https://doi.org/10.1016/j.chemosphere.
615 2007.01.002.

616 Hodson, A., Nowak, A., Holmlund, E.S., Redeker, K.R., Christiansen, H.H., 2019. Seasonal
617 Dynamics of Methane and Carbon Dioxide Evasion From an Open System Pingo: Lagoon
618 Pingo, Svalbard. Front. Earth Sci. 7, 30. https://doi.org/10.3389/feart.2019.00030.

619 Hu, B.B., Wang, D.Q., Zhou, J., Meng, W.Q., Li, C.W., Sun, Z.B., Guo, X., Wang, Z.L.,
620 2018. Greenhouse gases emission from the sewage draining rivers. Sci. Total Environ.
621 612, 1454−1462. https://doi.org/10.1016/j.scitotenv.2017.08.055.

622 Huttunen, J.T., Vaisanen, T.S., Hellsten, S.K., Heikkinen, M., Nykanen, H., Jungner, H.,
623 Niskanen, A., Virtanen, M.O., Lindqvist, O.V., Nenonen, O.S., Martikainen, P.J., 2002.
624 Fluxes of CH_4, CO_2, and N_2O in hydroelectric reservoirs Lokka and Porttipahta in the
625 northern boreal zone in Finland. Glob. Biogeochem. Cy. 16, 1003. https://doi.org/
626 10.1029/2000GB001316.

627 Holgerson, M.A., 2015. Drivers of carbon dioxide and methane supersaturation in small,
628 temporary ponds. Biogeochemistry 124, 305−318. https://doi.org/10.1007/s10533 -015-
629 0099-y.

630 Jacinthe, P.A., Filippelli, G.M., Tedesco, L.P., Raftis, R., 2012. Carbon storage and
631 greenhouse gases emission from a fluvial reservoir in an agricultural landscape. Catena
632 94, 53−63. https://doi.org/10.1016/j.catena.2011.03.012.

633 Jonsson, A., Karlsson, J., Jansson, M., 2003. Sources of carbon dioxide supersaturation in
634 clearwater and humic lakes in northern sweden. Ecosystems 6, 224−235. https://doi.org/
635 10.1007/s10021-002-0200-y.

636 Kamjunke, N., Buettner, O., Jaeger, C.G., Marcus, H., Von Tuempling, W., Halbedel, S.,
637 Norf, H., Brauns, M., Baborowski, M., Wild, R., Borchardt, D., Weitere, M., 2013.
638 Biogeochemical patterns in a river network along a land use gradient. Environ. Monit.
639 Assess. 185, 9221−9236. https://doi.org/10.1007/s10661-013-3247-7.

640 Kaushal, S.S., Delaney-Newcomb, K., Findlay, S.E.G., Newcomer, T.A., Duan, S., Pennino,
641 M.J., Sivirichi, G.M., Sides-Raley, A.M., Walbridge, M.R., Belt, K.T., 2014.
642 Longitudinal patterns in carbon and nitrogen fluxes and stream metabolism along an
643 urban watershed continuum. Biogeochemistry 121, 23−44.
644 https://doi.org/10.1007/s10533-014-9979-9.

645 Kemenes, A., Forsberg, B.R., Melack, J.M., 2011. CO_2 emissions from a tropical
646 hydroelectric reservoir (balbina, brazil). J. Geophys. Res-Biogeosci. 116, G03004.
647 https://doi.org/10.1029/2010jg001465.

648 Kortelainen, P., Rantakari, M., Huttunen, J.T., Mattsson, T., Alm, J., Juutinen, S., Larmola,
649 T., Silvola, J., Martikainen, P.J., 2006. Sediment respiration and lake trophic state are
650 important predictors of large CO_2 evasion from small boreal lakes. Glob. Chang. Biol. 12,
651 1554–1567. https://doi.org/10.1111/j.1365-2486.2006.01167.x.

652 Kosten, S., Roland, F., Da Motta Marques, D.M.L., Van Nes, E.H., Mazzeo, N., Sternberg,
653 L.d.S.L., Scheffer, M., Cole, J.J., 2010. Climate-dependent CO_2 emissions from lakes.
654 Global Biogeochem. Cycles 24. http://doi.org/10.1029/2009gb003618.

655 Kunz, M.J., Wueest, A., Wehrli, B., Landert, J., Senn, D.B., 2011. Impact of a large tropical
656 reservoir on riverine transport of sediment, carbon, and nutrients to downstream wetlands.
657 Water Resour. Res. 47. http://doi.org/10.1029/2011wr010996.

658 Kutzbach, L., Wille, C., Pfeiffer, E.M., 2007. The exchange of carbon dioxide between wet
659 arctic tundra and the atmosphere at the lena river delta, northern siberia. Biogeosciences
660 4, 869–890. http://doi.org/10.5194/bg-4-869-2007.

661 Lai, L., Huang, X., Yang, H., Chuai, X., Zhang, M., Zhong, T., Chen, Z., Chen, Y., Wang,
662 X., Thompson, J., R, 2016. Carbon emissions from land-use change and management in
663 China between 1990 and 2010. Sci. Adv. 2(11), e1601063. http://doi.org/10.1126/
664 sciadv.1601063.

665 Lehner, B., Liermann, C.R., Revenga, C., Voeroesmarty, C., Fekete, B., Crouzet, P., Doell,
666 P., Endejan, M., Frenken, K., Magome, J., Nilsson, C., Robertson, J.C., Roedel, R.,
667 Sindorf, N., Wisser, D., 2011. High-resolution mapping of the world's reservoirs and
668 dams for sustainable river-flow management. Front. Ecol. Environ. 9, 494–502.
669 http://doi.org/ 10.1890/100125.

670 Li, S., Lu, X.X., 2012. Uncertainties of carbon emission from hydroelectric reservoirs. Nat.
671 Hazards 62, 1343–1345. http://doi.org/10.1007/s11069-012-0127-3.

Li, S., Lu, X.X., Bush, R.T., 2013. CO_2 partial pressure and CO_2 emission in the lower mekong river. J. Hydrol. 504, 40–56. http://doi.org/10.1016/j.jhydrol.2013.09.024.

Li, S.Y., Zhang, Q.F., 2014. Partial pressure of CO_2 and CO_2 emission in a monsoon-driven hydroelectric reservoir (Danjiangkou Reservoir), China. Ecol. Eng. 71, 401–414. https://doi.org/10.1016/j.ecoleng.2014.07.014.

Li, Z., Zhang, Z., Lin, C., Chen, Y., Wen, A., Fang, F., 2016. Soil-air greenhouse gas fluxes influenced by farming practices in reservoir drawdown area: A case at the three gorges reservoir in china. J. Environ. Manag. 181, 64–73. http://doi.org/10.1016/j.jenvman.2016.05.080.

Li, S.Y., Bush, R.T., Santos, I.R., Zhang, Q.F., Song, K.S., Mao, R., Wen, Z.D., Lu, X.X., 2018. Large greenhouse gases emissions from China's lakes and reservoirs. Water Res. 147, 13–24. https://doi.org/10.1016/j.watres.2018.09.053.

Li, Y., Yang, H., Zhang, L., Yang, X., Zang, H., Fan, W., Wang, G., 2020a. The spatiotemporal variation and control mechanism of surface *p*CO2 in winter in Jiaozhou Bay, China. Cont. Shelf Res. 206. https://doi.org/10.1016/j.csr.2020.104208.

Li, Y., Zhang, L., Xue, L., Fan, W., Liu, F., Yang, H., 2020b. Spatial Variation in Aragonite Saturation State and the Influencing Factors in Jiaozhou Bay, China. Water 12(3), 825. https://doi.org/10.3390/w12030825.

Liu, H.P., Zhang, Q.Y., Katul, G.G., Cole, J.J., Chapin, F.S., MacIntyre, S., 2016. Large CO_2 effluxes at night and during synoptic weather events significantly contribute to CO_2 emissions from a reservoir. Environ. Res. Lett. 11(6), 8–10. https://doi.org/1088/ 1748-9326/11/6/064001.

Liu, Z., Guan, D.B., Crawford-Brown, D., Zhang, Q., He, K.B., Liu, J.G., 2013. A low-carbon road map for China. Nature 500(7461), 143–145. https://doi.org/10.1038/500143a.

Marescaux, A., Thieu, V., Garnier, J., 2018. Carbon dioxide, methane and nitrous oxide emissions from the human-impacted Seine watershed in France. Sci. Total Environ. 643, 247–259. https://doi.org/10.1016/j.scitotenv.2018.06.151.

Matthews, C.J.D., Joyce, E.M., St Louise, V.L., Schiff, S.L., Venkiteswaran, J.J., Hall, B.D., Bodaly, R.A., Beaty, K.G., 2005. Carbon dioxide and methane production in small reservoirs flooding upland boreal forest. Ecosystems 8, 267–285. http://doi.org/10.1007/s10021-005-0005-x.

Natchimuthu, S., Selvam, B.P., Bastviken, D., 2014. Influence of weather variables on methane and carbon dioxide flux from a shallow pond. Biogeochemistry 119, 403–413. http://doi.org/10.1007/s10533-014-9976-z.

Natchimuthu, S., Sundgren, I., Gålfalk, M., Klemedtsson, L., Crill, P., Danielsson, Å., Bastviken, D., 2016. Spatio-temporal variability of lake CH4 fluxes and its influence on annual whole lake emission estimates. Limnol. Oceanogr. 61, S13–S26. https://doi.org/10.1002/lno.10222.

Ni, M., Li, S., Luo, J., Lu, X., 2019. CO_2 partial pressure and CO_2 degassing in the daning river of the upper yangtze river, china. J. Hydrol. 569, 483–494. https://doi.org/10.1016/j.jhydrol.2018.12.017.

Nilsson, C., Reidy, C.A., Dynesius, M., Revenga, C., 2005. Fragmentation and flow regulation of the world's large river systems. Science 308, 405–408. http://doi.org/10.1126/science.1107887.

716 Outram, F.N., Hiscock, K.M., 2012. Indirect nitrous oxide emissions from surface water
717 bodies in a lowland arable catchment: A significant contribution to agricultural
718 greenhouse gas budgets? Environ. Sci. Technol. 46, 8156–8163. http://doi.org/
719 10.1021/es3012244.

720 Pacheco, F.S., Soares, M.C.S., Assireu, A.T., Curtarelli, M.P., Roland, F., Abril, G., Stech,
721 J.L., Alvala, P.C., Ometto, J.P., 2015. The effects of river inflow and retention time on
722 the spatial heterogeneity of chlorophyll and water-air CO_2 fluxes in a tropical hydropower
723 reservoir. Biogeosciences 12, 147–162. http://doi.org/10.5194/bg-12-147-2015.

724 Pérez, C.A., Degrandpre, M.D., Lagos, N.A., Saldías, G.S., Cascales, E.-K., Vargas, C.A.,
725 2015. Influence of climate and land use in carbon biogeochemistry in lower reaches of
726 rivers in central southern chile: Implications for the carbonate system in river-influenced
727 rocky shore environments. J. Geophys. Res-Biogeo. 120, 673–692. http://doi.org/
728 10.1002/2014jg002699.

729 Pugh, T.A.M., Arneth, A., Olin, S., Ahlstrom, A., Bayer, A.D., Goldewijk, K.K., Lindeskog,
730 M., Schurgers, G., 2015. Simulated carbon emissions from land-use change are
731 substantially enhanced by accounting for agricultural management. Environ. Res. Lett.
732 10. http://doi.org/10.1088/1748-9326/10/12/124008.

733 Raymond, P.A., Cole, J.J., 2003. Increase in the export of alkalinity from north america's
734 largest river. Science 301, 88–91. http://doi.org/10.1126/science.1083788.

735 Raymond, P.A., Hartmann, J., Lauerwald, R., Sobek, S., Mcdonald, C., Hoover, M., Butman,
736 D., Striegl, R., Mayorga, E., Humborg, C., Kortelainen, P., Duerr, H., Meybeck, M.,
737 Ciais, P., Guth, P., 2014. Global carbon dioxide emissions from inland waters. Nature
738 503, 355. http://doi.org/10.1038/nature13142.

739 Roland, F., Vidal, L.O., Pacheco, F.S., Barros, N.O., Assireu, A., Ometto, J.P.H.B.,
740 Cimbleris, A.C.P., Cole, J.J., 2010. Variability of carbon dioxide flux from tropical
741 (Cerrado) hydroelectric reservoirs. Aquat. Sci. 72, 283–293. https://doi.org/10.1007/
742 s00027-010-0140-0.

743 Rosenberg, D.M., Mccully, P., Pringle, C.M., 2000. Global-scale environmental effects of
744 hydrological alterations: Introduction. Bioscience 50, 746–751. http://doi.org/10.1641/
745 0006-3568(2000)050[0746:Gseeoh]2.0.Co;2.

746 Schilder, J., Bastviken, D., van Hardenbroek, M,. Kankaala, P., Rinta, P., Stotter, T., Heiri,
747 O., 2013. Spatial heterogeneity and lake morphology affect diffusive greenhouse gas
748 emission estimates of lakes. Geophys. Res. Lett. 40, 5752–5756. https://doi.org/
749 10.1002/2013GL057669.

750 Scofield, V., Melack, J.M., Barbosa, P.M., Amaral, J.H.F., Forsberg, B.R., Farjalla, V.F.,
751 2016. Carbon dioxide outgassing from amazonian aquatic ecosystems in the negro river
752 basin. Biogeochemistry 129, 77–91. http://doi.org/10.1007/s10533-016-0220-x.

753 Shi, W., Chen, Q., Yi, Q., Yu, J., Ji, Y., Hu, L., Chen, Y., 2017. Carbon emission from
754 cascade reservoirs: Spatial heterogeneity and mechanisms. Environ. Sci. Technol. 51,
755 12175–12181. http://doi.org/10.1021/acs.est.7b03590.

756 Sobek, S., Tranvik, L.J., Cole, J.J., 2005. Temperature independence of carbon dioxide
757 supersaturation in global lakes. Global Biogeochem. Cycles 19, GB2003.
758 http://doi.org/10.1029/2004gb002264.

759 Soumis, N., Lucotte, M., Larose, C., Veillette, F., Canuel, R., 2007. Photomineralization in a
760 boreal hydroelectric reservoir: A comparison with natural aquatic ecosystems.
761 Biogeochemistry 86, 123–135. http://doi.org/10.1007/s10533-007-9141-z.

762 St Louis, V.L., Kelly, C.A., Duchemin, E., Rudd, J.W.M., Rosenberg, D.M., 2000. Reservoir
763 surfaces as sources of greenhouse gases to the atmosphere: A global estimate. Bioscience
764 50, 766–775. http://doi.org/10.1641/0006-3568(2000)050[0766:Rsasog]2.0.Co;2.

765 Tong, C., Wang, W.Q., Zeng, C.S., Marrs, R., 2010. Methane (CH_4) emission from a tidal
766 marsh in the min river estuary, southeast china. J. Environ. Sci. Heal. A. 45, 506–516.
767 http://doi.org/10.1080/10934520903542261.

768 Urabe, J., Iwata, T., Yagami, Y., Kato, E., Suzuki, T., Hino, S., Ban, S., 2011. Within-lake
769 and watershed determinants of carbon dioxide in surface water: A comparative analysis of
770 a variety of lakes in the japanese islands. Limnol. Oceanogr. 56, 49–60.
771 http://doi.org/10.4319/lo.2011.56.1.0049.

772 Varis, O., Kummu, M., Härkönen, S., Huttunen, J.T., 2011. Greenhouse gas emissions from
773 reservoirs. Impacts of Large Dams: A Global Assessment, Springer 69–94.
774 https://doi.org/10.1007/978-3-642-23571-9_4.

775 Van Bergen, T.J.H.M., Barros, N., Mendonca, R., Aben, R.C.H., Althuizen, I.H.J., Huszar,
776 V., Lamers, L.P.M., Lurling, M., Roland, F., Kosten, S., 2019. Seasonal and diel variation
777 in greenhouse gas emissions from an urban pond and its major drivers. Limnol. Oceanogr.
778 64, 2129–2139. http://doi.org/10.1002/lno.11173.

779 Venkiteswaran, J.J., Schiff, S.L., Wallin, M.B., 2014. Large carbon dioxide fluxes from head-
780 water boreal and sub-boreal streams. PLoS One 9:22–25. https://doi.org/10.1371/
781 journal.pone.0101756.

782 Wang, F., Wang, B., Liu, C.-Q., Wang, Y., Guan, J., Liu, X., Yu, Y., 2011. Carbon dioxide
783 emission from surface water in cascade reservoirs-river system on the maotiao river,
784 southwest of China. Atmos. Environ. 45, 3827–3834. http://doi.org/10.1016/
785 j.atmosenv.2011.04.014.

786 Wang, X.F., He, Y.X., Yuan, X.Z., Chen, H., Peng, C.H., Yue, J.S., Zhang, Q.Y., Diao, Y.B.,
787 Liu, S.S., 2017. Greenhouse gases concentrations and fluxes from subtropical small
788 reservoirs in relation with watershed urbanization. Atmos. Environ. 154, 225–235.
789 http://doi.org/10.1016/j.atmosenv.2017.01.047.

790 Wanninkhof, R., 1992. Relationship between wind-speed and gas-exchange over the ocean. J.
791 Geophys. Res-Oceans. 97, 7373–7382. http://doi.org/10.1029/92jc00188.

792 Wanninkhof, R., 2014. Relationship between wind speed and gas exchange over the ocean
793 revisited. Limnol. Oceanogr-Meth. 12, 351–362. http://doi.org/10.4319/lom.2014. 12.351.

794 Webb, J.R., Santos, I.R., Tait, D.R., Sippo, J.Z., Macdonald, B.C.T., Robson, B., Maher,
795 D.T., 2016. Divergent drivers of carbon dioxide and methane dynamics in an agricultural
796 coastal floodplain: Post-flood hydrological and biological drivers. Chem. Geol. 440, 313–
797 325. http://doi.org/10.1016/j.chemgeo.2016.07.025.

798 Williams, C.J., Frost, P.C., Morales-Williams, A.M., Larson, J.H., Richardson, W.B.,
799 Chiandet, A.S., Xenopoulos, M.A., 2016. Human activities cause distinct dissolved
800 organic mattercomposition across freshwater ecosystems. Glob. Chang. Biol. 22, 613–
801 626. http://doi.org/10.1111/gcb.13094.

Wilson, B.J., Mortazavi, B., Kiene, R.P., 2015. Spatial and temporal variability in carbon dioxide and methane exchange at three coastal marshes along a salinity gradient in a northern gulf of mexico estuary. Biogeochemistry 123, 329–347. http://doi.org/10.1007/s10533-015-0085-4.

World Meteorological Organization, 2019. WMO Greenhouse Gas Bulletin No.15.

Xiao, Q.T., Zhang, M., Hu, Z.H., Gao, Y.Q., Hu, C., Liu, C., Liu, S.D., Zhang, Z., Zhao, J.Y., Xiao, W., Lee, X., 2017. Spatial variations of methane emission in a large shallow eutrophic lake in subtropical climate. J. Geophys. Res.-Biogeo. 122, 1597–1614. https://doi.org/10.1002/2017jg003805.

Xiao, S., Wang, Y., Liu, D., Yang, Z., Lei, D., Zhang, C., 2013. Diel and seasonal variation of methane and carbon dioxide fluxes at site guojiaba, the three gorges reservoir. J. Environ. Sci. 25, 2065–2071. https://doi.org/10.1016/s1001-0742(12)60269-1.

Xing, Y.P., Xie, P., Yang, H., Ni, L.Y., Wang, Y.S., Tang, W.H., 2004. Diel variation of methane fluxes in summer in a eutrophic subtropical lake in China. J. Freshwater Ecol. 19(4), 639–644. https://doi.org/10.1080/02705060.2004.9664745.

Xing, Y., Xie, P., Yang, H., Ni, L., Wang, Y., Rong, K., 2005. Methane and carbon dioxide fluxes from a shallow hypereutrophic subtropical Lake in China. Atmos. Environ. 39(30), 5532–5540. https://doi.org/10.1016/j.atmosenv.2005.06.010.

Xing, Y.P., Xie, P., Yang, H., Wu, A.P., Ni, L.Y., 2006. The change of gaseous carbon fluxes following the switch of dominant producers from macrophytes to algae in a shallow subtropical lake of China. Atmos. Environ. 40(40), 8034–8043. https://doi.org/10.1016/j.atmosenv.2006.05.033.

Yang, H., 2014. China must continue the momentum of green law. Nature 509, 535–535. https://doi.org/10.1038/509535a.

Yang, H., Andersen, T., Dörsch, P., Tominaga, K., Thrane, J.-E., Hessen, D.O., 2015. Greenhouse gas metabolism in Nordic boreal lakes. Biogeochemistry 126, 211–225. https://doi.org/10.1007/s10533-015-0154-8.

Yang, H., Flower, R.J., 2012. Potentially massive greenhouse-gas sources in proposed tropical dams. Front. Ecol. Environ. 10(5), 234–235. https://doi.org/10.1890/12.WB.014.

Yang, H., Flower, R.J., Thompson, J.R., 2013. China's new leaders offer green hope. Nature 493(7431), 163–163. https://doi.org/10.1038/493163d.

Yang, H., Huang, X., Thompson, J.R., Flower, R.J., 2015. Enforcement key to China's environment. Science 347(6224), 834–835. https://doi.org/10.1126/science.347.6224.834-d.

Yang, H., Ma, M., Thompson, J.R., Flower, R.J., 2017. Protect coastal wetlands in China to save endangered migratory birds. P. Natl. Acad. Sci. USA. 114(28), E5491–E5492. https://doi.org/10.1073/pnas.1706111114.

Yang, H., Thompson, J.R., Flower, R.J., 2019. Save horseshoe crabs and coastal ecosystems. Science 366(6467), 813–814. https://doi.org/10.1126/science.aaz8654.

Yang, H., Wright, J.A., Gundry, S.W., 2012a. Boost water safety in rural China. Nature 484(7394), 318–318. https://doi.org/10.1038/484318b.

Yang, H., Xie, P., Ni, L., Flower, R.J., 2012b. Pollution in the Yangtze. Science 337(6093), 410–410. https://doi.org/10.1126/science.337.6093.410-a.

Yang, H., Xing, Y., Xie, P., Ni, L., Rong, K., 2008. Carbon source/sink function of a subtropical, eutrophic lake determined from an overall mass balance and a gas exchange and carbon burial balance. Environ. Pollut. 151, 559–568. https://doi.org/10.1016/j.envpol.2007.04.006.

Yang, P., Zhang, Y., Lai, D.Y.F., Tan, L., Jin, B., Tong, C., 2018. Fluxes of carbon dioxide and methane across the water-atmosphere interface of aquaculture shrimp ponds in two subtropical estuaries: The effect of temperature, substrate, salinity and nitrate. Sci. Total Environ. 635, 1025–1035. https://doi.org/10.1016/j.scitotenv.2018.04.102.

Yang, P., Yang, H., Sardans, J., Tong, C., Zhao, G.H., Peñuelas, J., Li, L., Zhang, Y.F., Tan, L.S., Chun, K.P., Lai. D.Y.F., 2020. Large spatial variations in diffusive CH_4 fluxes from a subtropical coastal reservoir affected by sewage discharge in southeast China. Environ. Sci. Technol. 54, 22, 14192–14203. https://doi.org/10.1021/acs.est.0c03431

Yoon, T.K., Jin, H., Begum, M.S., Kang, N., Park, J. H., 2017. CO_2 outgassing from an urbanized river system fueled by wastewater treatment plant effluents. Environ. Sci. Technol. 51, 10459–10467. https://doi.org/10.1021/acs.est.7b02344.

Yu, Z., Wang, D., Li, Y., Deng, H., Hu, B., Ye, M., Zhou, X., Da, L., Chen, Z., Xu, S., 2017. Carbon dioxide and methane dynamics in a human-dominated lowland coastal river network (shanghai, china). Journal of Geophysical Research-Biogeosciences 122, 1738–1758. https://doi.org/10.1002/2017jg003798.

Zhang, M., Huang, X., Chuai, X., Yang, H., Lai, L., Tan, J., 2015. Impact of land use type conversion on carbon storage in terrestrial ecosystems of China: A spatial-temporal perspective. Sci. Rep-UK. 5, 10233. https://doi.org/10.1038/srep10233.

Zhang, Y.F, Yang, P., Yang, H., Tan, L.S, Guo, Q.Q, Zhao, G.H, Li, L., Gao, Y., Tong, C., 2019. Plot-scale spatiotemporal variations of CO_2 concentration and flux across water-air interfaces at aquaculture shrimp ponds in a subtropical estuary. Environ. Sci. Pollut. R. 26, 5623–5637. http://doi.org/10.1007/s11356-018-3929-3.

Zhao, Y., Wu, B.F., Zeng, Y., 2013. Spatial and temporal patterns of greenhouse gas emissions from three gorges reservoir of china. Biogeosciences 10, 1219–1230. http://doi.org/ 10.5194/bg-10-1219-2013.

Zhou, S., He, Y., Yuan, X., Peng, S., Yue, J., 2017. Greenhouse gas emissions from different land-use areas in the littoral zone of the three gorges reservoir, china. Ecol. Eng. 100, 316–324. http://doi.org/10.1016/j.ecoleng.2017.01.003.